

---

# Optimally adaptive Bayesian spectral density estimation for stationary and nonstationary processes

Nick James · Max Menzies

25 February 2021

**Abstract** This article improves on existing methods to estimate the spectral density of stationary and nonstationary time series assuming a Gaussian process prior. By optimising an appropriate eigendecomposition using a smoothing spline covariance structure, our method more appropriately models both smooth and rough data. We further justify the utility of this optimal eigendecomposition by investigating the performance of alternative covariance functions other than smoothing splines. We show that the optimal eigendecomposition provides a material improvement, while the other covariance functions under examination do not, all performing comparatively well as the smoothing spline. During our computational investigation, we introduce new validation metrics for the spectral density estimate, inspired from the physical sciences. We validate our models in an extensive simulation study and demonstrate superior performance with real data.

**Keywords** Spectral density estimation · nonstationary · reversible jump · Markov chain Monte Carlo · Gaussian process

## 1 Introduction

Spectral density estimation (SDE) is the key technique for understanding the autocovariance structure of a sta-

tionary time series. Of particular importance in the physical sciences, such as mass spectrometry [30,29], are the peaks of a power spectrum, and the frequencies at which they occur. However, most real-world processes are nonstationary. This has necessitated the development of methods for SDE for nonstationary time series. In this article, we improve upon existing techniques to estimate time-varying power spectra.

Our analysis takes place in a nonparametric Bayesian framework and implements an appropriately optimised *reversible jump Markov chain Monte Carlo* (RJMCMC) algorithm, assuming a *Gaussian process* (GP) prior. Aligning with the existing literature on locally stationary time series [7,1], we partition a given time series into a finite number of stationary segments. The true log power spectrum is estimated within the Whittle likelihood framework [34], using the local log periodograms.

Our key improvement over existing RJMCMC techniques is the optimisation of an appropriate eigendecomposition, where a smoothing spline covariance structure is used. Therein, we maximise the Whittle likelihood with respect to the number of eigenvalues. This produces a suitable estimate of the power spectrum for both smooth and rough data. To demonstrate the robustness of this smoothing spline optimisation, we also investigate alternative GP covariance functions. We specify to the stationary case and validate our estimates against analytically known autoregressive (AR) processes. We show that other covariance functions provide no benefit over the eigendecomposition of the smoothing spline. In the process thereof, we introduce new validation metrics that more appropriately reflect the needs of the physical sciences, where the amplitude and frequency of the peaks is paramount.

Our article builds off a rich history of nonparametric Bayesian modelling to analyse and fit data. First,

---

N. James  
School of Mathematics and Statistics  
The University of Sydney  
NSW, 2006, Australia  
E-mail: nicholas.james@sydney.edu.au

M. Menzies  
Yau Mathematical Sciences Center  
Tsinghua University  
Beijing, 100084, China  
E-mail: max.menzies@alumni.harvard.edu

smoothing splines are the bedrock for such analysis. Coghburn and Davis [6] and Wahba [31] pioneered the use of smoothing splines for spectral density estimation in the stationary case, with improvements made by Gandgopadhyay et al. [11], Choudhuri et al. [5] and others [37]. Guo et al. [14] used smoothing spline ANOVA in the locally stationary case. Variations of smoothing splines, such as B-splines [10], P-splines [38] and others [32, 13], have been used across a range of implementations in the statistics literature.

Alternative covariance functions for GPs, other than smoothing splines, have been used in a wide range of applications to model and analyse data. Rasmussen and Williams [24] provide an overview of modelling complex phenomena with combinations of covariance functions in GPs. Paciorek and Schervish [22] perform GP regression and investigate smoothness over a class of nonstationary covariance functions, while Plagemann et al. [23] utilise such functions within a Bayesian regression framework. More recently, nonparametric regression methods with automatic kernel learning have produced a GP regression framework for kernel learning [8], and other frameworks [20, 35]. However, alternative covariance functions have been used infrequently for the problem of SDE.

More recently, smoothing splines and GPs have been used to study the spectra of nonstationary processes. Whereas the work of Wahba [31] and Carter and Kohn [4] places priors over spectra of stationary processes, more recent work has extended this to nonstationary time series, predicated on the work of Dahlhaus [7] and Adak [1]. Reversible jump MCMC algorithms have been used to partition nonstationary time series into stationary segments. The number and location of these can be estimated flexibly from the data, and the uncertainty quantified, both in the time [36] and frequency domain [26, 28].

In particular, Rosen, Wood and Stoffer have used a smoothing spline GP covariance structure and RJMCMC algorithms in conjunction effectively to perform SDE in the nonstationary setting. Their work partitions nonstationary time segments into locally stationary segments, first with predetermined partitions [26] and then adaptively [28], in each case using a product of local Whittle likelihoods to estimate the time series' time-varying power spectrum. The model includes a particular eigendecomposition of the covariance matrix associated to the smoothing spline. For computational savings, the first 10 eigenvectors are used - this number is fixed.

The main limitation of the aforementioned work is the global degree of smoothness induced by the fixed eigendecomposition. In our article's experiments, we show that this model generally underfits real-world pro-

cesses. These usually exhibit more complexity than the autoregressive processes that are canonically used in the validation of such SDE models. This leads to a systemic bias in the literature towards models that produce excessively smooth spectral estimates. Indeed, Hadj-Amar et al. [15] examined the 10-eigenvector model of Rosen et al. [28] and concluded that the fixed decomposition tends to produce estimates that are overly smooth. Our article ameliorates this problem by varying the number of eigenvalues used and optimising it by maximising the Whittle likelihood. Quantitatively, we produce better results than other models as measured by new and existing validation metrics, and qualitatively, our estimates provide a more appropriate level of smoothness upon visual inspection.

The article is structured as follows: in Section 2, we introduce the mathematical model, including our key improvement. In Section 3, we describe our simulation study, incorporating both our chosen alternative covariance functions and introducing our new validation metrics. In Section 4, we apply our method to real data, and observe more appropriate fitting of our model to rough real-world data. In Section 5, we summarise our findings regarding the performance and appropriate smoothness produced by eigendecomposition optimisation versus variation of covariance functions in our GP model.

## 2 Mathematical model

### 2.1 Spectral density estimation

Let  $(X_t)_{t=1, \dots, n}$  be a discrete real valued time series.

**Definition 1**  $(X_t)$  is stationary if

1. Each random variable  $X_t$  is integrable with a finite common mean  $\mu$  for each  $t$ . By subtracting the mean, we may assume henceforth  $\mu = 0$ .
2. The autocovariance  $\mathbb{E}[(X_t - \mu)(X_{t+k} - \mu)]$  is a function only of  $k$ , which we denote  $\gamma(k)$ .

Spectral analysis allows us to study the second-order properties of a stationary time series expressed in the autocovariance structure. The power spectral density function (PSD) is defined as follows:

$$f(\nu) = \sum_{k=-\infty}^{\infty} \gamma(k) \exp(-2\pi i \nu k), \text{ for } -\frac{1}{2} \leq \nu \leq \frac{1}{2}. \quad (1)$$

Most important are the *Fourier frequencies*  $\nu_j = \frac{j}{n}$ ,  $j = 0, 1, \dots, n-1$ . Define the *discrete Fourier transform* (DFT) of the time series:

$$Z(\nu_j) = \frac{1}{\sqrt{n}} \sum_{t=1}^n X_t \exp(-2\pi i \nu_j t), \text{ for } j = 0, \dots, n-1.$$

(2)

Whittle initially showed that under certain conditions, the DFTs have a *complex normal* (CN) distribution [34, 33]:

$$\mathbf{Z} \sim \text{CN}(\mathbf{0}, \mathbf{F}), \text{ where } \mathbf{F} = \text{diag}[f(\nu_0), \dots, f(\nu_{n-1})]. \quad (3)$$

For each Fourier frequency component, a noisy but unbiased estimate of the PSD  $f(\nu_k)$  is the *periodogram* [5], defined by  $I(\nu_j) = |Z(\nu_j)|^2$ . By symmetry, the periodogram contains  $m = \lfloor \frac{n}{2} \rfloor + 1$  effective observations, corresponding to  $j = 0, 1, \dots, m-1$ . Rosen et al. [26, 28] outline a signal plus noise representation of the periodogram:

$$\log I(\nu_j) = \log f(\nu_j) + \epsilon_j, \text{ where } \epsilon_j \sim \log(\exp(1)). \quad (4)$$

Indeed, for a wide class of theoretical models, Theorem 10.3.2 of [3] proves that the vector of quotients

$$\left( \frac{I(\nu_0)}{f(\nu_0)}, \dots, \frac{I(\nu_{m-1})}{f(\nu_{m-1})} \right) \quad (5)$$

converges in distribution to a vector of independent and identically distributed (i.i.d.)  $\exp(1)$  random variables.

For our applications, we assume the quotient  $\frac{I}{f}$  is approximately exponentially distributed with mean 1. This is a simpler representation of the second moment of the distribution, reducing the problem of covariance estimation to a simpler problem of mean estimation. Note the periodogram oscillates around the true spectral density, so there is a delicate balance between inferring the spectrum of a process and excessive smoothing, leading to negligible inference.

## 2.2 Gaussian process regression

**Definition 2** A *Gaussian process* is a collection of random variables, any finite collection of which have a multivariate Gaussian distribution [24]. Such a process  $f(\mathbf{x})$  is uniquely determined by its mean function  $m(\mathbf{x}) = \mathbb{E}[f(\mathbf{x})]$  and covariance function  $k(\mathbf{x}, \mathbf{x}') = \mathbb{E}[(f(\mathbf{x}) - m(\mathbf{x}))(f(\mathbf{x}') - m(\mathbf{x}'))]$ . We write  $f(\mathbf{x}) \sim \mathcal{GP}(m(\mathbf{x}), k(\mathbf{x}, \mathbf{x}'))$ .

We assume the standard “noisy observation” Gaussian additive error model  $y = f(\mathbf{x}) + \epsilon$ , in which  $\epsilon$  is i.i.d Gaussian noise with variance  $\sigma_n^2$  [24]. Then, the prior over the noisy observations is  $\text{cov}(\mathbf{y}) = k(\mathbf{x}, \mathbf{x}') + \sigma_n^2 I$ . The joint distribution of observed response values,  $\mathbf{y}$ , and function values evaluated at test points under the prior distribution,  $\mathbf{f}_*$  is expressed as

$$\begin{bmatrix} \mathbf{y} \\ \mathbf{f}_* \end{bmatrix} \sim \mathcal{N} \left( \mathbf{0}, \begin{bmatrix} k(\mathbf{x}, \mathbf{x}) + \sigma_n^2 I & k(\mathbf{x}, \mathbf{x}_*) \\ k(\mathbf{x}_*, \mathbf{x}) & k(\mathbf{x}_*, \mathbf{x}_*) \end{bmatrix} \right).$$

Finally, the GP regression predictive equations are as follows [24]:

$$\mathbf{f}_* | \mathbf{x}, \mathbf{y}, \mathbf{x}' \sim \mathcal{N}(\bar{\mathbf{f}}_*, \text{cov}(\mathbf{f}_*)), \quad (6)$$

where the mean and covariance are defined as

$$\bar{\mathbf{f}}_* := \mathbb{E}[\mathbf{f}_* | \mathbf{x}, \mathbf{y}, \mathbf{x}_*] = k(\mathbf{x}_*, \mathbf{x}) [k(\mathbf{x}, \mathbf{x}) + \sigma_n^2 I]^{-1} \mathbf{y}, \quad (7)$$

$$\text{cov}(\mathbf{f}_*) := k(\mathbf{x}_*, \mathbf{x}_*) - k(\mathbf{x}_*, \mathbf{x}) [k(\mathbf{x}, \mathbf{x}) + \sigma_n^2 I]^{-1} k(\mathbf{x}, \mathbf{x}_*). \quad (8)$$

## 2.3 Model and priors

We follow [5, 28] and use the Whittle likelihood function to model the log periodogram within a Bayesian regression framework. Let  $\mathbf{y} = (y(\nu_0), \dots, y(\nu_{m-1}))$  be the log of the periodogram,  $\mathbf{f} = (f(\nu_0), \dots, f(\nu_{m-1}))$  be the PSD, and  $\mathbf{g} = (g(\nu_0), \dots, g(\nu_{m-1}))$  be the log of the PSD. The likelihood of the log periodogram given the true power spectrum can be approximated by

$$p(\mathbf{y} | \mathbf{f}) = (2\pi)^{-m/2} \prod_{j=0}^{m-1} \exp \left( -\frac{1}{2} \left[ \log f(\nu_j) + \frac{I(\nu_j)}{f(\nu_j)} \right] \right). \quad (9)$$

Following [26, 28] we rewrite Eq. (4) as

$$y(\nu_j) = g(\nu_j) + \epsilon_j, \quad (10)$$

To obtain a flexible estimate of the spectrum, we place a GP prior over the unknown function  $\mathbf{g}$ . That is, we assume  $\mathbf{g} \sim N(\mathbf{0}, k(\mathbf{x}, \mathbf{x}_*))$ . This is determined by its covariance function. Most of the SDE literature to date has used smoothing splines [31] or other spline varieties for this covariance structure. In subsequent sections, we investigate both smoothing splines and other covariance functions. We choose kernels that have been frequently examined elsewhere in the literature: the squared exponential, Matern<sub>3/2</sub>, Matern<sub>5/2</sub>, Sigmoid kernel, and combinations of these such as the squared exponential + Sigmoid [24, 22, 23, 20, 35].

## 2.4 MCMC implementation and choice of covariance functions

The primary contribution of this paper is an improved RJMCMC method for SDE of nonstationary time series. Our work builds on the RJMCMC of Rosen et al. [28], found in Appendix A. This scheme partitions the time series into locally stationary segments and models the log PSD  $\log f(\nu)$  of the segments with a Gaussian process with covariance matrix  $\Omega$ . For computational savings,

they employ an eigendecomposition  $\Omega = QDQ^T$  and retain only the 10 largest eigenvectors in  $D$ . That is, they let  $D_{10}$  be the truncated diagonal matrix and set  $X = QD_{10}^{1/2}$  as their design matrix. Let  $\beta$  be a vector of unknown regression coefficients with prior distribution  $N(0, \tau^2 I)$  (where  $\tau^2$  is a smoothing parameter). Then the successive estimate for the PSD is  $\log f(\nu) = X\beta$ , iterated within the RJMCMC.

Given that the eigendecomposition is so critical, the exact number of eigenvalues should be estimated using the data. Hard-coding a 10-eigenvalue decomposition yields a smoothing spline that may be too smooth or too rough depending on the process being estimated. If the true process is highly smooth, our estimator will exhibit too much variance; if the process is particularly rough, our estimator will exhibit excessive bias. Instead, we select an optimal number of eigenvalues  $M$  by analysing posterior samples of the log spectrum for a range of eigenvectors, integrating over all possible values of regression coefficients, and maximising the Whittle likelihood. We select our number of eigenvalues as follows:

$$\hat{M} = \operatorname{argmax}_{M \geq 1} \int p(\mathbf{y}|M, X_M, \beta) p(\beta|M, X_M) d\beta, \quad (11)$$

where  $\mathbf{y}$  is the log periodogram data,  $X_M$  is the design matrix under an eigendecomposition using  $M$  eigenvalues, and  $\beta$  is a vector of coefficients determining the weight for respective eigenvectors. We refer to the corresponding eigendecomposition  $\Omega = QD_{\hat{M}}Q^T$  as the *optimal smoothing spline*.

In subsequent sections, we examine the performance of the optimal smoothing spline against both simulated and real data. First, we specialise to the stationary case, where we may validate this optimal smoothing spline in the case of autoregressive processes with known analytic spectra. In this setting, there is no need for the partition of the time series, so the RJMCMC scheme reduces to a Metropolis-Hastings scheme described in Appendix B. In this implementation, we are also free to substitute alternative GP covariance functions  $k(\mathbf{x}, \mathbf{x}')$  (see Definition 2 and Appendix B). The optimal smoothing spline compares favourably not only to the 10-eigenvalue decomposition but also to the other covariance functions and provides further justification of its utility.

Having established that the optimal smoothing spline performs the best of our covariance functions in the stationary case, we proceed to a simulated nonstationary time series, once again using the RJMCMC. By examining three adjoined autoregressive processes with varying spectral complexity, we demonstrate the improvement in our method over the 10-eigenvalue decomposition by validating each segment against its known analytic

spectra. Finally, we proceed to test our optimal smoothing spline on real data, which is much less smooth than the autoregressive processes studied until this point. We show that the 10-eigenvalue decomposition drastically underfits the many peaks of more complex real-world data.

## 2.5 Validation metrics

In the subsequent simulation study, we use new and existing validation metrics to compare our spectral density estimates  $\hat{\mathbf{g}}$  of autoregressive processes with the known analytic log PSD  $\mathbf{g}$ . The three existing metrics we use are root mean squared error (RMSE), defined as  $\sqrt{\frac{1}{m} \sum_{j=0}^{m-1} (\hat{g}(\nu_j) - g(\nu_j))^2}$ , mean absolute error (MAE), defined as  $\frac{1}{m} \sum_{j=0}^{m-1} |\hat{g}(\nu_j) - g(\nu_j)|$ , and the Wasserstein distance between the finite sets  $\{g(\nu_j)\}$  and  $\{\hat{g}(\nu_j)\}$ . Specifically, this converts a finite set to a uniform probability measure over its elements and computes the Wasserstein distance between these measures (see [18], Definition 2.5 or [19], Section 2.1).

Our new validation metrics are inspired by applications in the physical sciences, where a single dominant peak is often the greatest importance to observing scientists [30]. Such a peak has two attributes, its amplitude,  $\max g$  and the frequency at which it occurs,  $\operatorname{argmax} g$ . With this in mind, we introduce two validation metrics,  $|\max \hat{g} - \max g|$  and  $|\operatorname{argmax} \hat{g} - \operatorname{argmax} g|$ , measuring how well the spectral density estimation determines the amplitude and frequency of the greatest peak.

Next, we consider the possibility of multiple peaks in an analytic or estimated power spectrum, as is the case for an AR(4) process. First, we consider the simplest possible case, assuming the following *a priori*:

1. the analytic and estimated power spectra have the same number of peaks,  $\rho_1, \dots, \rho_r$  for  $g$  and  $\hat{\rho}_1, \dots, \hat{\rho}_r$  for  $\hat{g}$ ;
2. there is a bijection between the two sets of peaks, for which each  $\rho_i$  is the closest peak of  $g$  to  $\hat{\rho}_i$ , and vice versa.

Informally, this is the ideal situation, in which the peaks of  $g$  can be matched one-to-one to their closest counterpart among the peaks of  $\hat{g}$ , and vice versa. In this ideal case, we can define a validation metric between peaks' collective amplitudes and frequencies, respectively, for any  $p \geq 1$  as follows:

$$\left( \frac{|g(\rho_1) - \hat{g}(\hat{\rho}_1)|^p + \dots + |g(\rho_r) - \hat{g}(\hat{\rho}_r)|^p}{r} \right)^{\frac{1}{p}}, \quad (12)$$

$$\left( \frac{|\rho_1 - \hat{\rho}_1|^p + \dots + |\rho_r - \hat{\rho}_r|^p}{r} \right)^{\frac{1}{p}}. \quad (13)$$

If  $p = 2$ , we return a (normalised) Euclidean distance between tuples  $(\rho_1, \dots, \rho_r)$  and  $(\hat{\rho}_1, \dots, \hat{\rho}_r) \in \mathbb{R}^r$ . If  $p = 1$ , we return an  $L^1$  distance between the tuples. In subsequent paragraphs, we will see why the normalisation is appropriate for a more general framework.

More generally, we wish to outline a framework that specifically tests for whether this bijection exists, and define a validation measure that is well-defined regardless of whether the bijection exists. For this purpose, let  $S$  be the finite set of the (non-trivial) peaks of an analytic power spectrum  $g$ , and  $\hat{S}$  be the set of (non-trivial) peaks of an estimate  $\hat{g}$ . The most naive definition of a peak as a local maximum of  $g$  or  $\hat{g}$ , respectively, may be unsuitable for this purpose - due to the wiggly nature of spectral density estimates, there may exist local maxima of  $\hat{g}$  that are insubstantial and should be excluded. An algorithmic framework for the refinement of peaks in the power spectra must be employed. A flexible algorithmic framework that does this for local maxima and minima can be found in [17]. Many approaches exist in this framework. For example, local maxima that are significantly less than other local maxima may be excluded as insubstantial under a variety of definitions and parameters. In our experiments with the AR(4) process, only a simple approach is needed: set  $\delta = 2$ ; any local maximum  $\hat{\rho}$  of  $\hat{g}$  with  $\hat{g}(\hat{\rho}) < \max \hat{g} - \delta$  is excluded. The same results are produced for any  $\delta \in [2, 4]$ , demonstrating the robustness of this refinement procedure.

Having determined such sets  $S$  and  $\hat{S}$  through a choice of parameters within such a framework, we define the *proximity matching criterion* as follows: say  $S$  and  $\hat{S}$  satisfy this criterion if:

1. there is a function  $f : S \rightarrow \hat{S}$ , where for each  $s \in S$ ,  $f(s)$  is the unique closest element of  $\hat{S}$  to  $s$ ;
2. there is a function  $\hat{f} : \hat{S} \rightarrow S$ , where conversely for each  $\hat{s} \in \hat{S}$ ,  $\hat{f}(\hat{s})$  is the unique closest element of  $S$  to  $\hat{s}$ ;
3. The functions  $f$  and  $\hat{f}$  are mutually inverse.

This criterion formalises the ideal case described above, where the (non-trivial) peaks of  $g$  and  $\hat{g}$  can be matched one-to-one and hence labelled  $\rho_1, \dots, \rho_r$  and  $\hat{\rho}_1, \dots, \hat{\rho}_r$  via the mutually inverse bijective functions  $f$  and  $\hat{f}$ . Independently of this criterion, we define a validation measure between sets  $S$  and  $\hat{S}$  as follows, adopting the *semi-metrics* defined in [18]:

$$d^p(S, \hat{S}) = \left( \frac{\sum_{\hat{s} \in \hat{S}} d(\hat{s}, S)^p}{2|\hat{S}|} + \frac{\sum_{s \in S} d(s, \hat{S})^p}{2|S|} \right)^{\frac{1}{p}}, \quad (14)$$

where  $d(\hat{s}, S)$  is the minimal distance from  $\hat{s}$  to  $S$ , and vice versa. This validation semi-metric can be applied to measure the collective distance between the sets of

peaks of an analytic and estimated spectra under any circumstance, conditional on an appropriate algorithmic selection of non-trivial peaks. Moreover, in the case where the proximity matching criterion is satisfied and the sets of peaks can be matched up and labelled as  $\rho_1, \dots, \rho_r$  and  $\hat{\rho}_1, \dots, \hat{\rho}_r$ , it simply reduces to the metric (13), together with its normalising factor, between tuples  $(\rho_1, \dots, \rho_r)$  and  $(\hat{\rho}_1, \dots, \hat{\rho}_r) \in \mathbb{R}^r$ .

To summarise, we have defined a general validation (semi)-metric between the collective sets of peaks of an analytic and estimated power spectra  $g$  and  $\hat{g}$ , respectively. For full generality and precision, the sets of peaks must be selected from the data with a flexible algorithmic framework suitable for the application at hand, and not merely chosen by observation from the shape of the analytic spectrum. In the most suitable case, this semi-metric will reduce to what is still a new validation metric defined in Eq. (13).

### 3 Simulation study

In this section, we study the properties of our estimators with a detailed simulation study. We simulate three stationary autoregressive processes, AR(1), AR(2) and AR(4), and validate our spectral density estimates against their known analytic power spectra. For each experiment, we run 50 simulations with our MCMC scheme, either RJMCMC or Metropolis-Hastings, as described in Section 2. Each sampling scheme consists of 10 000 iterations, with 5000 used for burn-in, and each process contains  $n = 500$  data points. Following the notation of Section 2, we set  $m = 251$  and consider Fourier frequencies  $\nu_j = \frac{j}{n}$ ,  $j = 0, 1, \dots, m - 1$ , the appropriate range of the periodogram and spectrum. As such, the range of the frequency axis in all plots is  $0 \leq \nu \leq \frac{1}{2}$ . Henceforth,  $\epsilon_t$  denotes a white noise random variable with distribution  $N(0, 1)$ .

First, we generate data from an AR(1) process  $x_t = 0.9x_{t-1} + \epsilon_t$ . We compute the log periodogram from the observed data and estimate the log PSD and GP hyperparameters with our MCMC scheme. Table 1 indicates that the best performing covariance functions are the squared exponential and Sigmoid. The log PSD has high power at low frequency and gradually declines in power when moving toward higher frequency components. The spectrum does not exhibit any sharp peaks and it is unsurprising that the highly smooth squared exponential performs well in estimating the log PSD. The worst performing covariance function is the 10-eigenvector decomposition of the smoothing spline of Rosen et al [28]. There is little improvement with the optimal smoothing spline model in this case, as seen in Figure 1a. This experiment suggests that for a simple spectrum, there is

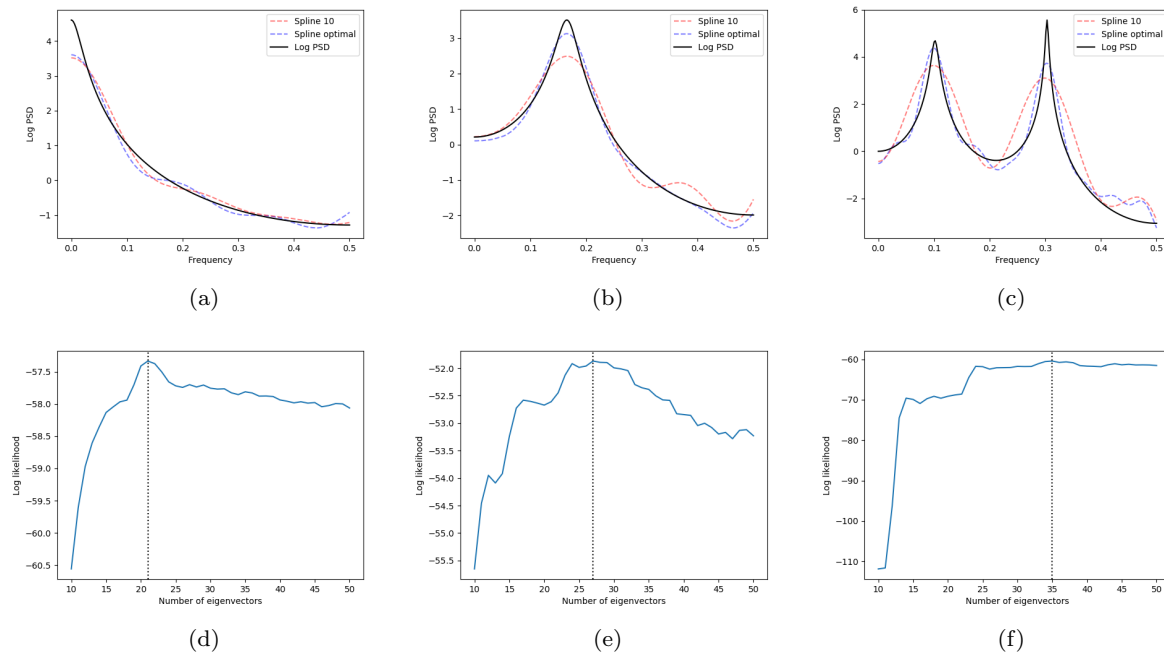


Fig. 1: Analytic and estimated log PSD for 10-eigenvector and optimal decomposition of the smoothing spline models for (a) AR(1) (b) AR(2) (c) AR(4). Log likelihood vs number of eigenvectors for (d) AR(1) (e) AR(2) and (f) AR(4) process. The peak in the log likelihood determines the number of eigenvectors in the optimal model.

limited improvement in optimising the number of basis functions in the smoothing spline and alternative GP covariance functions provide superior performance.

Next, we generate data from an AR(2) process  $x_t = 0.9x_{t-1} - 0.8x_{t-2} + \epsilon_t$ , compute the log periodogram and estimate the log PSD and GP hyperparameters with the MCMC schemes. Table 1 indicates that several covariance functions perform similarly well: SQE+Sigmoid, squared exponential, both Matern functions, and the optimal spline. The Sigmoid kernel and 10-eigenvector decomposition of the spline perform worse. The log PSD has a relatively flat gradient and a mild peak at  $\nu \sim 0.15$ . Once again, smoother covariance functions tend to perform better, while the Sigmoid covariance function, popularised for its ability to model abrupt changes in data modelling problems [24], is a poor performer. Figure 1b demonstrates a substantial improvement in estimating the log PSD when an optimal number, larger than 10, of basis functions is used. In particular, the estimator does a better job of detecting the maximum amplitude of the power spectrum.

Third, we follow [9], generate data from an AR(4) process  $x_t = 0.9x_{t-1} - 0.9x_{t-2} + 0.9x_{t-3} - 0.9x_{t-4} + \epsilon_t$ , and again estimate the log PSD and GP hyperparameters with the MCMC schemes. The log PSD of the AR(4) process is more complex than the prior two experiments. There are two peaks of different amplitudes in the spec-

trum, and the spectrum changes more abruptly than the AR(1) and AR(2) spectra. Table 1 indicates that the best performing covariance functions are the optimal smoothing spline and the two Matern functions. The worst performing covariance functions are the 10-eigenvector smoothing spline and the Sigmoid kernel. Once again we see a substantial improvement in estimation when an optimal number of basis functions is used, displayed in Figure 1c.

As the AR(4) process has two peaks, we may also test the proximity matching criterion of Section 2.5 and measure the distance between the collective sets of peaks of the estimated and analytic power spectra. In Table 2, we note that in this relatively simple example with just two peaks, all covariance functions satisfy this criterion. As such, the more general semi-metric (14) reduces to the simpler metric between frequencies (13). We also include the collective distance between amplitudes in the table, as defined in (12). These distances show that the optimal smoothing spline does the best job at estimating both peaks at the same time.

Figures 1d, 1e and 1f plot the Whittle likelihood against the number of eigenvectors for the AR(1), AR(2) and AR(4) processes, respectively - this selects the optimal number of basis functions for each. We see that consistently more than 10 basis functions are required to optimally model the data; in fact, the choice of 10

AR(1) model					
Covariance function	RMSE	MAE	Wasserstein	$ \operatorname{argmax} g - \operatorname{argmax} \hat{g} $	$ \max g - \max \hat{g} $
Spline <sub>10</sub>	0.26	0.20	0.18	0	0.90
Spline <sub>optimal</sub>	0.25	0.19	0.16	0	0.93
Squared exponential	0.16	0.12	0.12	0	0.49
Matern <sub>3/2</sub>	0.19	0.15	0.13	0	0.51
Matern <sub>5/2</sub>	0.19	0.14	0.12	0	0.49
Sigmoid	0.15	0.11	0.11	0	0.34
SQE+Sigmoid	0.18	0.14	0.13	0	0.40
AR(2) model					
Covariance function	RMSE	MAE	Wasserstein	$ \operatorname{argmax} g - \operatorname{argmax} \hat{g} $	$ \max g - \max \hat{g} $
Spline <sub>10</sub>	0.33	0.26	0.24	0.0020	0.73
Spline <sub>optimal</sub>	0.21	0.17	0.14	0.0020	0.36
Squared exponential	0.22	0.17	0.15	0.0020	0.56
Matern <sub>3/2</sub>	0.21	0.17	0.14	0.0020	0.24
Matern <sub>5/2</sub>	0.19	0.15	0.13	0.0020	0.37
Sigmoid	0.32	0.24	0.22	0.0040	0.85
SQE+Sigmoid	0.21	0.17	0.15	0.0020	0.53
AR(4) model					
Covariance function	RMSE	MAE	Wasserstein	$ \operatorname{argmax} g - \operatorname{argmax} \hat{g} $	$ \max g - \max \hat{g} $
Spline <sub>10</sub>	0.82	0.63	0.54	0.20	2.23
Spline <sub>optimal</sub>	0.43	0.33	0.26	0.20	1.57
Squared exponential	0.45	0.31	0.27	0.20	1.98
Matern <sub>3/2</sub>	0.37	0.27	0.21	0.20	1.75
Matern <sub>3/2</sub>	0.40	0.29	0.24	0.20	1.90
Sigmoid	0.97	0.75	0.41	0.21	2.12
SQE+Sigmoid	0.45	0.32	0.26	0.20	2.06

Table 1: Results for synthetic data experiments. Median error over 50 simulations is recorded for various covariance functions and validation metrics. Each MCMC scheme consists of 10,000 iterations where 5,000 are used for burn-in. For each AR process,  $n = 1000$ .

basis functions in the eigendecomposition is only really appropriate for the AR(1) and AR(2) spectrum. Even the synthetic AR(4) spectrum, but more so real-world processes, benefit from an optimised decomposition that can better suit their complexity and lack of smoothness. Indeed, real-world time series may have multiple periodic components represented in complex power spectra with multiple peaks, of varying amplitudes. The fixed 10-eigenvector decomposition is excessively smooth for these more complex spectra.

Finally, we include one last simulation study to demonstrate the efficacy of our improved RJMCMC at both segmenting a nonstationary time series and then estimating the power spectrum of each locally stationary segment. We generate a piecewise autoregressive time series by concatenating three AR processes of segment

length  $n = 500$ :

$$x_t = \begin{cases} 0.9x_{t-1} - 0.9x_{t-2} + -.9x_{t-3} - 0.9x_{t-4} + \epsilon_t, & 1 \leq t \leq 500; \\ 0.8x_{t-1} - 0.6x_{t-2} + \epsilon_t, & 501 \leq t \leq 1000; \\ 0.7x_{t-1} - 0.15x_{t-2} + 0.1x_{t-3} - 0.6x_{t-4} + \epsilon_t, & 1001 \leq t \leq 1500. \end{cases} \quad (15)$$

As before, we plot the Whittle likelihood against the number of eigenvectors in Figure 2a - this selects the optimal number of basis functions for the optimal smoothing spline. We remark that the optimal number of basis functions is computed by optimising over the entire time-varying spectral surface. This figure clearly demonstrates the need for optimising the number of eigenvectors. Indeed, the 10-eigenvector decomposition provides the lowest likelihood of the data, with 39 eigenvectors being optimal. Figures 2b, 2c and 2d show that the optimal

AR(4) process: distance between sets of peaks		
Covariance function	Proximity matching criterion	Amplitude distance
Spline <sub>10</sub>	Yes	1.64
Spline <sub>optimal</sub>	Yes	0.99
Squared exponential	Yes	1.24
Matern <sub>3/2</sub>	Yes	1.18
Matern <sub>5/2</sub>	Yes	1.31
Sigmoid kernel	Yes	1.57
SQE+Sigmoid	Yes	1.34

Table 2: Amplitude distance between collective sets of peaks of analytic and estimated AR(4) power spectra  $g$  and  $\hat{g}$ , respectively.

smoothing spline model provides improved performance over each segment.

In Figure 2b, the optimal smoothing spline more effectively captures abrupt peaks in the PSD. We remark that the slight overfitting exhibited by the optimal spline would not lead to erroneous inference, as this overfitting only occurs at frequency components with limited power. In Figure 2c, the optimal spline does a superior job at estimating both peaks in amplitude, while avoiding overfitting at frequency components that exhibit the most power. In Figure 2d, we see two peaks in the PSD with significantly varying amplitude. There, the optimal model more appropriately determines the amplitude and frequency of the greatest peaks, just like our validation metrics in Table 1 recorded.

Figures 2e and 2f display the two time-varying PSD estimated using the original 10-eigenvector decomposition and our optimal spline, respectively. Figure 2f clearly generates a more intricate surface than Figure 2e, which is inappropriately smooth. In particular, the scale of the  $z$ -axis demonstrates the optimised model’s improvement when estimating appropriate peaks at respective frequencies in the PSD.

## 4 Real data

In this section, we analyse the spectra of two canonical datasets, sunspots [5] and airline passenger data [2]. Both time series are well studied, with the former being particularly well studied in the spectral density estimation literature. We compare the performance of the optimal smoothing spline model and the 10-eigenvector smoothing spline. Unlike AR processes, real data do not possess analytic power spectra to validate estimates against. Both time series require transformations to ensure they are stationary. For the sunspots data, following Choudhuri [5], we perform the following transformation:

$$S_t = y_t^{\frac{1}{2}} - \mu(\{y_t^{\frac{1}{2}} : t = 1, \dots, n\}).$$

That is, we take the square root of the observations and then mean-centre the resulting values. For the airline passenger data, we perform an original transformation based on first differences of fourth roots:

$$A_t = y_t^{\frac{1}{4}} - y_{t-1}^{\frac{1}{4}}.$$

The two transformed time series are displayed in Figures 3a and 3b. As before, the number of basis functions is optimised to maximise the marginal Whittle likelihood. For the sunspots and airline passenger data respectively, the optimal number of basis functions is 24 and 49, seen in Figures 3c and 3d respectively.

Figures 3e and 3f demonstrate that our improved method models these complex processes substantially better than the existing 10-eigenvector model of Rosen et al. [28], and that the latter does not have the complexity to model such processes. In Figure 3e, the optimal smoothing spline captures the abruptness and amplitude of the one significant peak, as well as most of the movement of the log periodogram, while removing some of its characteristic noise. The 10-eigenvector spline fails to capture these features, with only slight recognition of that early peak. In Figure 3f, the optimal smoothing spline captures all five peaks of this spectrum and most of its complex undulating behaviour; the 10-eigenvector spline fails to capture the prominent peaks in the data or provide any meaningful or accurate inference of the spectrum.

## 5 Conclusion

This paper has proposed and demonstrated the use of an improved RJMCMC algorithm for spectral density estimation of stationary and nonstationary time series. In addition to performing better quantitatively with respect to new and existing metrics, we have shown significantly better performance at appropriately matching the abruptness and complexity present in the PSD

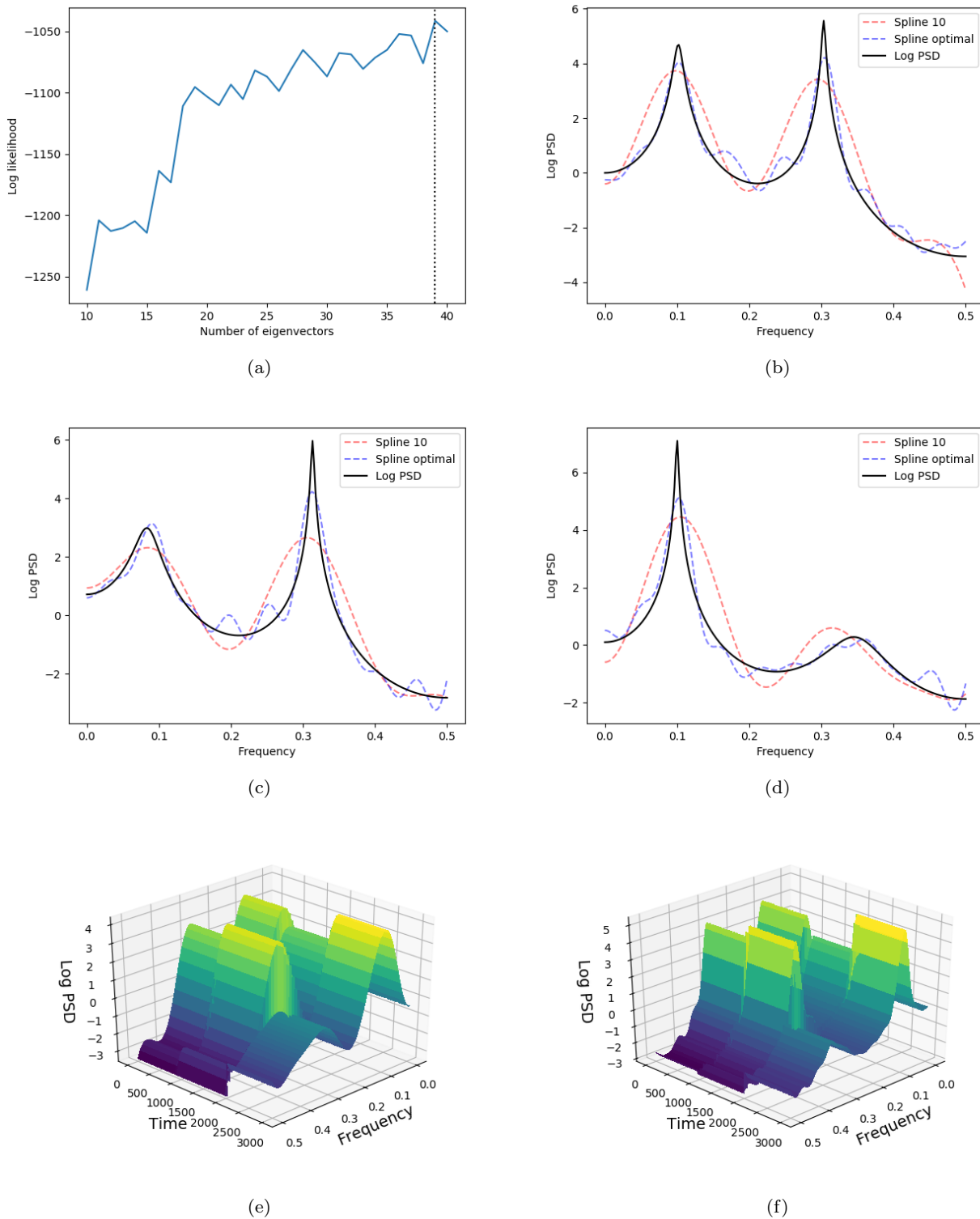


Fig. 2: Analytic and estimated log PSD for 10-eigenvector and optimal decomposition of smoothing spline models for nonstationary time series. (a) Log likelihood vs number of eigenvectors. Spectral estimates for (b) Segment 1 (c) Segment 2 (d) Segment 3. Spectral surface (time-varying PSD) for (e) 10-eigenvector and (f) optimal eigendecomposition.

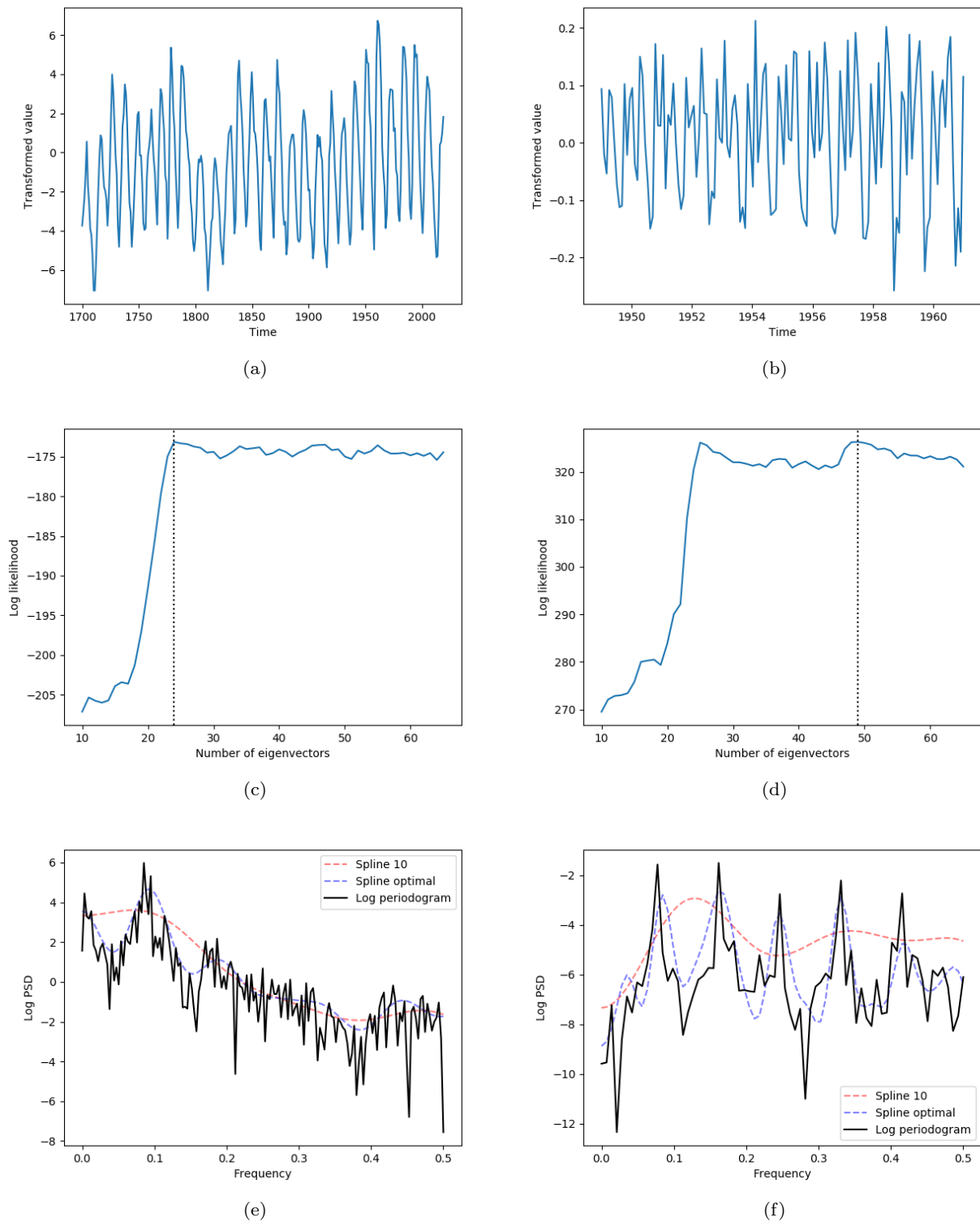


Fig. 3: Transformed time series for (a) sunspots (b) airline passenger data. Log likelihood vs number of eigenvectors for (c) sunspots (d) airline passenger data. Estimated log PSD for 10-eigenvector and optimal decomposition smoothing spline models for (e) sunspots (f) airline passenger data.

of real-world processes. The existing 10-eigenvector decomposition of Rosen et al. [28] appropriately models smooth processes like the AR(1) and AR(2), but substantially underfits the real data we have presented; our optimal smoothing spline has a greater capability to fit both smooth and abruptly changing spectra.

As further justification of the utility of the optimised eigendecomposition, we examine alternative covariance functions other than the smoothing spline and compare these against both the optimal and existing spline model in several settings. Our simulation study confirms that most well-known covariance functions perform acceptably well when analysing the power spectral density for stationary time series. Generally, smoother covariance functions such as the squared exponential and Matern perform better in the cases of smoother and simpler spectra, while models that combine stationary and nonstationary covariance functions such as the SQE+Sigmoid appear to generalise best across more complex spectral densities. The 10-eigenvector decomposition of the smoothing spline, as used within [28], is the worst performing model. In particular, we demonstrate that eigenvector optimisation is what constitutes improvement in this case, not alternative covariance functions. Simply put, given that the eigendecomposition is so critical, it really should be learned from the data.

There are a variety of interesting directions for future research. One could partition a locally stationary time series while at the same time optimising the number of basis functions used in the MCMC scheme within each segment, rather than over the entire time series period, as we have done. Future modelling frameworks could consider Bayesian and frequentist methods for identifying and learning the most appropriate covariance functions, or combinations thereof, to use within each segment of the time series. This could be performed within a Bayesian or non-Bayesian framework. We could also combine the eigendecomposition with the other covariance functions we have explored, including a learned choice of best covariance function through model averaging. Finally, our new validation metrics focused on collective sets of peaks, including the proximity matching criterion and algorithms for the appropriate refinement of peaks, could be employed in other contexts. These could be used together to measure a model's effectiveness at specifically identifying a set of multiple peaks arising from more complex data.

**Acknowledgements** Many thanks to Lamiae Azizi, Sally Cripps and Alex Judge for helpful discussions.

## Conflict of interest

The authors declare that they have no conflict of interest.

## Appendix A Reversible jump sampling scheme

We follow Rosen et al. [27,28] in our core implementation of the reversible jump sampling scheme. A time series partition is denoted  $\xi_m = (\xi_{0,m}, \dots, \xi_{m,m})$  with  $m$  segments. We have a vector of *amplitude parameters*  $\tau_m^2 = (\tau_{1,m}^2, \dots, \tau_{m,m}^2)'$  and *regression coefficients*  $\beta_m = (\beta'_{1,m}, \dots, \beta'_{m,m})$  that we wish to estimate, for the  $j$ th component within a partition of  $m$  segments,  $j = 1, \dots, m$ . For notational simplicity,  $\beta_j, m, j = 1, \dots, m$ , is assumed to include the first entry,  $\alpha_{0j,m}$ . In the proceeding sections superscripts  $c$  and  $p$  refer to current and proposed value in the sampling scheme.

First, we describe the **between-model moves**: let  $\theta_m = (\xi'_m, \tau_m^2, \beta'_m)$  be the model parameters at some point in the sampling scheme and assume that the chain starts at  $(m^c, \theta_{m^c}^c)$ . The algorithm proposes the move to  $(m^p, \theta_{m^p}^p)$ , by drawing  $(m^p, \theta_{m^p}^p)$  from the proposal distribution  $q(m^p, \theta_{m^p}^p | m^c, \theta_{m^c}^c)$ . That draw is accepted with probability

$$\alpha = \min \left\{ 1, \frac{p(m^p, \theta_{m^p}^p | \mathbf{x}) q(m^c, \theta_{m^c}^c | m^p, \theta_{m^p}^p)}{p(m^c, \theta_{m^c}^c | \mathbf{x}) q(m^p, \theta_{m^p}^p | m^c, \theta_{m^c}^c)} \right\},$$

with  $p(\cdot)$  referring to a target distribution, the product of the likelihood and the prior. The target and proposal distributions will vary based on the type of move taken in the sampling scheme. First,  $q(m^p, \theta_{m^p}^p | m^c, \theta_{m^c}^c)$  is described as follows:

$$\begin{aligned} q(m^p, \theta_{m^p}^p | m^c, \theta_{m^c}^c) &= q(m^p | m^c) q(\theta_{m^p}^p | m^p, m^c, \theta_{m^c}^c) \\ &= q(m^p | m^c) q(\xi_{m^p}^p, \tau_{m^p}^{2p}, \beta_{m^p}^p | m^p, m^c, \theta_{m^c}^c) \\ &= q(m^p | m^c) q(\xi_{m^p}^p | m^p, m^c, \theta_{m^c}^c) q(\tau_{m^p}^{2p} | \xi_{m^p}^p, m^p, m^c, \theta_{m^c}^c) \\ &\quad \times q(\beta_{m^p}^p | \tau_{m^p}^{2p}, \xi_{m^p}^p, m^p, m^c, \theta_{m^c}^c). \end{aligned}$$

To draw  $(m^p, \theta_{m^p}^p)$  one must first draw  $m^p$ , followed by  $\xi_{m^p}^p$ ,  $\tau_{m^p}^{2p}$ , and  $\beta_{m^p}^p$ . First, the number of segments  $m^p$  is drawn from the proposal distribution  $q(m^p | m^c)$ . Let  $M$  be the maximum number of segments and  $m_{2,\min}^c$  be the number of current segments whose cardinality is at least  $2m_{\min}$  data points. The proposal is as follows:

$$q(m^p = k | m^c) = \begin{cases} 1/2 & \text{if } k = m^c - 1, m^c + 1 \text{ and } m^c \neq 1, M, m_{2,\min}^c \neq 0 \\ 1 & \text{if } k = m^c - 1 \text{ and } m^c = M \text{ or } m_{2,\min}^c = 0 \\ 1 & \text{if } k = m^c + 1 \text{ and } m^c = 1 \end{cases}$$

Conditional on the proposed model  $m^p$ , a new partition  $\xi_{m^p}^p$ , a new vector of covariance amplitude parameters  $\tau_{m^p}^{2p}$ , and a new vector of regression coefficients,  $\beta_{m^p}^p$  are proposed. In [28],  $\tau^2$  is referred to as a smoothing parameter. To impact the smoothness of the covariance function, the parameter would have to impact pairwise operations. Given that  $\tau^2$  sits outside the covariance matrix, we will refer to  $\tau^2$  as an amplitude parameter (akin to signal variance within the Gaussian process framework [24]).

Now, we describe the process of the **birth** of new segments. Suppose that  $m^p = m^c + 1$ . A time series partition,

$$\xi_{m^p}^p = (\xi_{0,m^c}^c, \dots, \xi_{k^*-1,m^c}^c, \xi_{k^*,m^p}^p, \xi_{k^*,m^c}^c, \dots, \xi_{m^c,m^c}^c)$$

is drawn from the proposal distribution  $q(\xi_{m^p}^p | m^p, m^c, \theta_{m^c}^c)$ . The algorithm proposes a partition by first selecting a random segment  $j = k^*$  to split. Then, a point  $t^*$  within the segment  $j = k^*$  is randomly selected to be the proposed partition point. This is subject to the constraint,  $\xi_{k^*-1, m^c}^c + t_{\min} \leq t^* \leq \xi_{k^*, m^c}^c - t_{\min}$ . The proposal distribution is computed as follows:

$$q(\xi_{j, m^p}^p = t^* | m^p, m^c, \xi_{m^c}^c) = p(j = k^* | m^p, m^c, \xi_{m^c}^c) \\ p(\xi_{k^*, m^p}^p = t^* | j = k^*, m^p, m^c, \xi_{m^c}^c) \\ = \frac{1}{m_{2\min}^c (n_{k^*, m^c} - 2t_{\min} + 1)}.$$

The vector of amplitude parameters

$$\tau_{m^p}^{2p} = (\tau_{1, m^c}^{2c}, \dots, \tau_{k^*-1, m^c}^{2c}, \\ \tau_{k^*, m^p}^{2p}, \tau_{k^*+1, m^p}^{2p}, \tau_{k^*+1, m^c}^{2c}, \dots, \tau_{m^c}^{2c})$$

is drawn from the proposal distribution  $q(\tau_{m^p}^{2p} | m^p, \xi_{m^p}^p, m^c, \theta_{m^c}^c) = q(\tau_{m^p}^{2p} | m^p, \tau_{m^c}^{2c})$ . The algorithm is based on the reversible jump algorithm of Green [12]. It draws from a uniform distribution  $u \sim U[0, 1]$  and defines  $\tau_{k^*, m^p}^{2p}$  and  $\tau_{k^*+1, m^p}^{2p}$  in terms of  $u$  and  $\tau_{k^*, m^c}^{2c}$  as follows:

$$\tau_{k^*, m^p}^{2p} = \frac{u}{1-u} \tau_{k^*, m^c}^{2c}; \quad (16) \\ \tau_{k^*+1, m^p}^{2p} = \frac{1-u}{u} \tau_{k^*, m^c}^{2c}. \quad (17)$$

The vector of coefficients

$$\beta_{m^p}^p = (\beta_{1, m^c}^c, \dots, \beta_{k^*-1, m^c}^c, \\ \beta_{k^*, m^p}^p, \beta_{k^*+1, m^p}^p, \beta_{k^*+1, m^c}^c, \dots, \beta_{m^c}^c)$$

is drawn from the proposal distribution  $q(\beta_{m^p}^p | \tau_{m^p}^{2p}, \xi_{m^p}^p, m^p, m^c, \theta_{m^c}^c) = q(\beta_{m^p}^p | \tau_{m^p}^{2p}, \xi_{m^p}^p, m^p)$ . The pair of vectors  $\beta_{k^*, m^p}^p$  and  $\beta_{k^*+1, m^p}^p$  are drawn from Gaussian approximations to the respective posterior conditional distributions  $p(\beta_{k^*, m^p}^p | \mathbf{x}_{k^*}^p, \tau_{k^*, m^p}^{2p}, m^p)$  and  $p(\beta_{k^*+1, m^p}^p | \mathbf{x}_{k^*+1}^p, \tau_{k^*+1, m^p}^{2p}, m^p)$ , respectively. Here,  $\mathbf{x}_{k^*}^p$  and  $\mathbf{x}_{k^*+1}^p$  refer to the subsets of the time series with respective segments  $k^*$  and  $k^* + 1$ .  $\xi_{m^p}^p$  will determine  $\mathbf{x}_{k^*}^p = (\mathbf{x}_{k^*}^p, \mathbf{x}_{k^*+1}^p)'$ . For the sake of exposition, we provide the following example: the coefficient  $\beta_{k^*, m^p}^p$  is drawn from the Gaussian distribution  $N(\beta_{k^*}^{\max}, \Sigma_{k^*}^{\max})$ , where  $\beta_{k^*}^{\max}$  is defined as

$$\operatorname{argmax}_{\beta_{k^*, m^p}^p} p(\beta_{k^*, m^p}^p | \mathbf{x}_{k^*}^p, \tau_{k^*, m^p}^{2p}, m^p)$$

and

$$\Sigma_{k^*}^{\max} = - \left\{ \frac{\partial^2 \log p(\beta_{k^*, m^p}^p | \mathbf{x}_{k^*}^p, \tau_{k^*, m^p}^{2p}, m^p)}{\partial \beta_{k^*, m^p}^p \partial \beta_{k^*, m^p}^p} \right\}_{\beta_{k^*, m^p}^p = \beta_{k^*}^{\max}}^{-1}.$$

For the birth move, the probability of acceptance is  $\alpha = \min\{1, A\}$ , where  $A$  is equal to

$$\left| \frac{\partial(\tau_{k^*, m^p}^{2p}, \tau_{k^*+1, m^p}^{2p})}{\partial(\tau_{k^*, m^c}^{2c}, u)} \right| \frac{p(\theta_{m^p}^p | \mathbf{x}, m^p) p(\theta_{m^p}^p | m^p) p(m^p)}{p(\theta_{m^p}^c | \mathbf{x}, m^p) p(\theta_{m^c}^c | m^c) p(m^c)} \\ \times \frac{p(m^c | m^p) p(\beta_{k^*, m^c}^c)}{p(m^p | m^c) p(\xi_{k^*, m^p}^p | m^p, m^c) p(u) p(\beta_{k^*, m^p}^p) p(\beta_{k^*+1, m^p}^p)}.$$

Above,  $p(u) = 1, 0 \leq u \leq 1$ , while  $p(\beta_{k^*, m^p}^p)$  and  $p(\beta_{k^*+1, m^p}^p)$  are Gaussian proposal distributions  $N(\beta_{k^*}^{\max}, \Sigma_{k^*}^{\max})$  and  $N(\beta_{k^*+1}^{\max}, \Sigma_{k^*+1}^{\max})$ , respectively. The Jacobian is computed as

$$\left| \frac{\partial(\tau_{k^*, m^p}^{2p}, \tau_{k^*+1, m^p}^{2p})}{\partial(\tau_{k^*, m^c}^{2c}, u)} \right| = \frac{2\tau_{k^*, m^c}^{2c}}{u(1-u)} = 2(\tau_{k^*, m^p}^{2p} + \tau_{k^*+1, m^p}^{2p})^2.$$

Next, we describe the process of the **death** of new segments, that is, the reverse of a birth move, where  $m^p = m^c - 1$ . A time series partition

$$\xi_{m^p}^p = (\xi_{0, m^c}^c, \dots, \xi_{k^*-1, m^c}^c, \xi_{k^*+1, m^c}^c, \dots, \xi_{m^c}^c),$$

is proposed by randomly selecting a single partition from  $m^c - 1$  candidates, and removing it. The partition point selected for removal is denoted  $j = k^*$ . There are  $m^c - 1$  possible segments available for removal among the  $m^c$  segments currently in existence. The proposal may choose each partition point with equal probability, that is,

$$q(\xi_{j, m^p}^p | m^p, m^c, \xi_{m^c}^c) = \frac{1}{m^c - 1}.$$

The vector of amplitude parameters

$$\tau_{m^p}^{2p} = (\tau_{1, m^c}^{2c}, \dots, \tau_{k^*-1, m^c}^{2c}, \tau_{k^*, m^p}^{2c}, \tau_{k^*+2, m^c}^{2c}, \dots, \tau_{m^c}^{2c})$$

is drawn from the proposal distribution

$q(\tau_{m^p}^{2p} | m^p, \xi_{m^p}^p, m^c, \theta_{m^c}^c) = q(\tau_{m^p}^{2p} | m^p, \tau_{m^c}^{2c})$ . One amplitude parameter  $\tau_{k^*, m^p}^{2p}$  is formed from two candidate amplitude parameters,  $\tau_{k^*, m^c}^{2c}$  and  $\tau_{k^*+1, m^c}^{2c}$ . This is done by reversing the equations 16 and 17. That is,

$$\tau_{k^*, m^p}^{2p} = \sqrt{\tau_{k^*, m^c}^{2c} \tau_{k^*+1, m^c}^{2c}}.$$

Finally, the vector of regression coefficients,

$$\beta_{m^p}^p = (\beta_{1, m^c}^c, \dots, \beta_{k^*-1, m^c}^c, \beta_{k^*, m^p}^p, \beta_{k^*+2, m^c}^c, \dots, \beta_{m^c}^c)$$

is drawn from the proposal distribution

$q(\beta_{m^p}^p | \tau_{m^p}^{2p}, \xi_{m^p}^p, m^p, m^c, \theta_{m^c}^c) = q(\beta_{m^p}^p | \tau_{m^p}^{2p}, \xi_{m^p}^p, m^p)$ . The vector of regression coefficients is drawn from a Gaussian approximation to the posterior distribution  $p(\beta_{k^*, m^p}^p | \mathbf{x}_{k^*}^p, \tau_{k^*, m^p}^{2p}, \xi_{m^p}^p, m^p)$  following the same procedure for the vector of coefficients in the birth step. The probability of acceptance is the inverse of the analogous birth step. If the move is accepted then the following updates occur:  $m^c = m^p$  and  $\theta_{m^c}^c = \theta_{m^p}^p$ .

Finally, we describe the **within-model moves**: henceforth,  $m$  is fixed; accordingly, notation describing the dependence on the number of segments is removed. There are two parts to a within-model move. First, a segment relocation is performed, and conditional on the relocation, the basis function coefficients are updated. The steps are jointly accepted or rejected with a Metropolis-Hastings step. The amplitude parameters are updated within a separate Gibbs sampling step.

The chain is assumed to be located at  $\theta^c = (\xi^c, \beta^c)$ . The proposed move  $\theta^p = (\xi^p, \beta^p)$  is as follows: first, a partition point  $\xi_{k^*}$  is selected for relocation from  $m - 1$  candidate partition points. Next, a position within the interval  $[\xi_{k^*-1}, \xi_{k^*+1}]$  is selected, subject to the fact that the new location is at least  $t_{\min}$  data points away from  $\xi_{k^*-1}$  and  $\xi_{k^*+1}$ , so that

$$\Pr(\xi_{k^*}^p = t) = \Pr(j = k^*) \Pr(\xi_{k^*}^p = t | j = k^*),$$

where  $\Pr(j = k^*) = (m - 1)^{-1}$ . A mixture distribution for  $\Pr(\xi_{k^*}^p = t | j = k^*)$  is constructed to explore the space most efficiently, so

$$\Pr(\xi_{k^*}^p = t | j = k^*) = \pi q_1(\xi_{k^*}^p = t | \xi_{k^*}^c) + (1 - \pi) q_2(\xi_{k^*}^p = t | \xi_{k^*}^c),$$

where  $q_1(\xi_{k^*}^p = t | \xi_{k^*}^c) = (n_{k^*} + n_{k^*+1} - 2t_{\min} + 1)^{-1}$ ,  $\xi_{k^*-1} + t_{\min} \leq t \leq \xi_{k^*+1} - t_{\min}$  and

$$q_2(\xi_{k^*}^p = t | \xi_{k^*}^c) = \begin{cases} 0 & \text{if } |t - \xi_{k^*}^c| > 1 \\ 1/3 & \text{if } |t - \xi_{k^*}^c| \leq 1, n_{k^*} \neq t_{\min} \text{ and } n_{k^*+1} \neq t_{\min} \\ 1/2 & \text{if } |t - \xi_{k^*}^c| \leq 1, n_{k^*} = t_{\min} \text{ and } n_{k^*+1} \neq t_{\min} \\ 1/2 & \text{if } \xi_{k^*}^c - t \leq 1, n_{k^*} \neq t_{\min} \text{ and } n_{k^*+1} = t_{\min} \\ 1 & \text{if } t = \xi_{k^*}^c, n_{k^*} = t_{\min} \text{ and } n_{k^*+1} = t_{\min} \end{cases}$$

The support of  $q_1$  has  $n_{k^*} + n_{k^*+1} - 2t_{\min} + 1$  data points while  $q_2$  has at most three. The term  $q_2$  alone would result in a high acceptance rate for the Metropolis-Hastings, but it would explore the parameter space slowly. The  $q_1$  component allows for larger jumps, and produces a compromise between a high acceptance rate and thorough exploration of the parameter space.

Next,  $\beta_j^p, j = k^*, k^* + 1$  is drawn from an approximation to  $\prod_{j=k^*}^{k^*+1} p(\beta_j | \mathbf{x}_j^p, \tau_j^2)$ , following the analogous step in the between-model move. The proposal distribution, which is evaluated at  $\beta_j^p, j = k^*, k^* + 1$ , is

$$q(\beta_*^p | \mathbf{x}_*^p, \tau_*^2) = \prod_{j=k^*}^{k^*+1} q(\beta_j^p | \mathbf{x}_j^p, \tau_j^2),$$

where  $\beta_*^p = (\beta_{k^*}^p, \beta_{k^*+1}^p)'$  and  $\tau_*^2 = (\tau_{k^*}^2, \tau_{k^*+1}^2)'$ . The proposal distribution is evaluated at current values of  $\beta_*^c = (\beta_{k^*}^c, \beta_{k^*+1}^c)'$ .  $\beta_*^p$  is accepted with probability

$$\alpha = \min \left\{ 1, \frac{p(\mathbf{x}_*^p | \beta_*^p) p(\beta_*^p | \tau_*^2) q(\beta_*^c | \mathbf{x}_*^c, \tau_*^2)}{p(\mathbf{x}_*^c | \beta_*^c) p(\beta_*^c | \tau_*^2) q(\beta_*^p | \mathbf{x}_*^p, \tau_*^2)} \right\},$$

where  $\mathbf{x}_*^c = (\mathbf{x}_{k^*}^c, \mathbf{x}_{k^*+1}^c)$ . When the draw is accepted, update the partition and regression coefficients  $(\xi_{k^*}^c, \beta_*^c) = (\xi_{k^*}^p, \beta_*^p)$ . Finally, draw  $\tau^{2p}$  from

$$p(\tau_*^2 | \beta_*) = \prod_{j=k^*}^{k^*+1} p(\tau_j^2 | \beta_j).$$

This is a Gibbs sampling step, and accordingly the draw is accepted with probability 1.

## Appendix B Metropolis-Hastings algorithm

In this section, we describe the Metropolis-Hastings algorithm used in the stationary case for our simulation study (Section 3). As seen in Appendix A, the above RJMCMC reduces to a Metropolis-Hastings in the absence of the between-model moves.

We estimate the log of the spectral density by its posterior mean via a Bayesian approach and an adaptive MCMC algorithm:

$$\mathbb{E}(\mathbf{g} | \mathbf{y}) = \int \mathbb{E}(\mathbf{g} | \mathbf{y}, \theta) p(\theta | \mathbf{y}) d\theta \simeq \frac{1}{M} \sum_{j=1}^M \mathbb{E}(\hat{\mathbf{g}} | \mathbf{y}, \theta^j). \quad (18)$$

Here,  $M$  is the number of post burn-in iterations in the MCMC scheme;  $\theta^j$  are samples taken from the posterior distribution  $p(\theta | \mathbf{y})$ ;  $p(\theta)$  is taken from a Gaussian distribution  $N(\mu, \sigma^2)$  centred around  $\mu = \theta^{[c]}$  that maximises the log marginal likelihood;  $\sigma$  is chosen arbitrarily; and  $\hat{\mathbf{g}}$  is the forecast log spectrum.

Monte Carlo algorithms have been highly prominent for estimation of hyperparameters and spectral density in a nonparametric Bayesian framework. Metropolis [21] first proposed the Metropolis algorithm; this was generalised by Hastings in a more focused, statistical context [16]. The random walk Metropolis-Hastings algorithm aims to sample from a target density  $\pi$ , given some candidate transition probability function  $q(x, y)$ . In our context,  $\pi$  represents the Whittle likelihood function multiplied by respective priors. The acceptance ratio is:

$$\alpha(x, y) = \begin{cases} \min \left( \frac{\pi(y)q(y, x)}{\pi(x)q(x, y)}, 1 \right) & \text{if } \pi(x)q(x, y) > 0 \\ 1 & \text{if } \pi(x)q(x, y) = 0. \end{cases} \quad (19)$$

Our MCMC scheme calculates the acceptance ratio every 50 iterations; based on an ideal acceptance ratio [25], the step size is adjusted for each hyperparameter. The power spectrum and hyperparameters for the GP covariance function are calculated in each iteration of our sampling scheme and integrated over.

First, we initialise the values of our GP hyperparameters,  $\theta^{[c]}$ , our log PSD  $\hat{g}^c$ , our random perturbation size  $s^2$ , and the adaptive adjustment for our step size  $\xi$ . Starting values for our GP hyperparameters are chosen based on maximising the marginal Whittle likelihood,

$$\theta^{[c]} = \underset{\theta}{\operatorname{argmax}} - (2\pi)^{-m/2} \prod_{j=0}^{m-1} \exp \left( -\frac{1}{2} \left[ \log f(\nu_j) + \frac{I(\nu_j)}{f(\nu_j)} \right] \right). \quad (20)$$

The latent log PSD is modelled with a zero mean GP, That is,  $\mathbf{g} \sim GP(0, k_{\theta}(x, x'))$ , and we follow the notation of [24] where  $k(x, x')$  refers to any respective kernel. The adaptive MCMC algorithm samples from the posterior distribution of the log PSD and the posterior distribution of any candidate covariance function's hyperparameters. First, the current and proposed values for the mean and covariance of the Gaussian process are computed. That is, the mean is computed:

$$\hat{g}^c = k_{\theta^c}(x', x) [k_{\theta^c}(x, x) + \sigma^2 I]^{-1} \log I(\nu), \quad (21)$$

and the covariance is computed:

$$\hat{V}^c = k_{\theta^c}(x', x') - k_{\theta^c}(x', x) [k_{\theta^c}(x, x) + \sigma^2 I]^{-1} k_{\theta^c}(x, x'). \quad (22)$$

New proposals for GP hyperparameters are determined via a random walk proposal distribution. A zero-mean Gaussian distribution is used to generate candidate perturbations, where  $s^2$  is the variance of this Gaussian. That is

$$\theta^p \leftarrow q(\theta^p | \theta^c). \quad (23)$$

Having drawn the proposed GP hyperparameters, a proposed mean and covariance function of the log PSD are drawn from the posterior distribution of the GP. Both the proposed mean and covariance are computed similarly to the current values, simply replacing the values of the hyperparameters  $\theta^c \leftarrow \theta^p$ . So, the proposed mean of the log PSD is,

$$\hat{g}^p = k_{\theta^p}(x', x) [k_{\theta^p}(x, x) + \sigma^2 I]^{-1} \log I(\nu) \quad (24)$$

and the proposed covariance is computed as follows

$$\hat{V}^p = k_{\theta^p}(x', x') - k_{\theta^p}(x', x)[k_{\theta^p}(x, x) + \sigma^2 I]^{-1} k_{\theta^p}(x, x'). \quad (25)$$

Having computed the proposed and current values of the log PSD, we update the current log PSD based on the Metropolis-Hastings transition kernel. First, we sample from a uniform distribution  $u \sim U(0, 1)$  and compute our acceptance ratio,

$$\alpha = \min \left( 1, \frac{p(\log I(\nu) | \theta^p, \hat{g}^p) p(\hat{g}^p) q(\hat{g}^c | \log I(\nu), \theta^p)}{p(\log I(\nu) | \theta^c, \hat{g}^c) p(\hat{g}^c) q(\hat{g}^p | \log I(\nu), \theta^c)} \right). \quad (26)$$

$p(\log I(\nu) | \theta^p, \hat{g}^p)$  is our Whittle likelihood computation, the probability of the log PSD conditional on hyperparameters  $\theta$  and our candidate estimate of the latent log PSD  $\hat{g}$ .  $p(\hat{g}^p)$  represents the prior distribution on our latent log PSD and  $q(\hat{g}^c | \log I(\nu), \theta^p)$  is our proposal distribution, representing the probability of the estimated log PSD conditional on the log periodogram and GP hyperparameters.

Should  $u < \alpha$ , we update the current values of the log PSD mean and spectrum to the proposed values. That is,

$$\hat{g}^{c+1} \leftarrow \hat{g}^p \quad (27)$$

$$\hat{V}^{c+1} \leftarrow \hat{V}^p. \quad (28)$$

If  $u > \alpha$ , both the mean and variance of the log PSD are kept at their current values,

$$\hat{g}^{c+1} \leftarrow \hat{g}^c \quad (29)$$

$$\hat{V}^{c+1} \leftarrow \hat{V}^c. \quad (30)$$

Importantly, modelling the log PSD with a GP prior does not mean that we are assuming a Gaussian error distribution around the spectrum. In actuality, proposed spectra are accepted and rejected through a Metropolis-Hastings procedure - resulting in log PSD samples being drawn from the true posterior distribution of the log PSD,  $\log(\exp(1))$ . Having sampled the log PSD, we then accept/reject candidate GP hyperparameters with another Metropolis-Hastings step. Our acceptance ratio is,

$$\alpha = \min \left( 1, \frac{p(\log I(\nu) | \theta^p) p(\theta^c | \theta^p)}{p(\log I(\nu) | \theta^c) p(\theta^p | \theta^c)} \right), \quad (31)$$

where  $p(\log I(\nu) | \theta)$  represents the Whittle likelihood modelling the probability of the log PSD,  $\log I(\nu)$ , conditional on hyperparameters  $\theta$ .  $p(\theta^p | \theta)$  is the prior distribution we place over GP hyperparameters,  $\theta$ . Note that in this particular case, the symmetric proposal distributions cancel out and our algorithm reduces simply to a Metropolis ratio. Again we follow the standard Metropolis-Hastings acceptance decision. If  $u < \alpha$ ,

$$\theta^{c+1} \leftarrow \theta^p, \quad (32)$$

and the current hyperparameter values assume proposed values. Alternatively, if  $u > \alpha$ ,

$$\theta^{c+1} \leftarrow \theta^c, \quad (33)$$

current value of the hyperparameters are not updated. Finally, following [25] we implement an adaptive step-size within our random walk proposal. Every 50 iterations within our simulation, we compute the trailing acceptance ratio. An optimal acceptance ratio,  $\text{Acc}^{\text{Opt}}$  of 0.234 is targeted. If the

acceptance ratio is too low, indicating that the step size may be too large, then the step size is systematically reduced. If  $\text{Acceptance Ratio}_{(j-49):j} \forall j \in \{50, 100, 150, \dots, 10000\} < \text{Acc}^{\text{Opt}}$ ,

$$s^2 \leftarrow s^2 - \xi. \quad (34)$$

If the acceptance ratio is too high, indicating that the step size may be too small then step size is systematically increased. That is, when  $\text{Acceptance Ratio}_{(j-49):j} \forall j \in \{50, 100, \dots, 10000\} > \text{Acc}^{\text{Opt}}$ ,

$$s^2 \leftarrow s^2 + \xi. \quad (35)$$

Finally, the log PSD and the respective analytic uncertainty bounds are determined by computing the median of the samples generated from the sampling procedure,

$$\mathcal{U}_{0.025}^{\text{final}} = \text{median}(\mathcal{U}_{0.025}^{5000:10000}) \quad (36)$$

$$\hat{g} = \text{median}(\hat{g}^{5000:10000}) \quad (37)$$

$$\mathcal{U}_{0.975}^{\text{final}} = \text{median}(\mathcal{U}_{0.975}^{5000:10000}). \quad (38)$$

## References

1. Adak, S.: Time-dependent spectral analysis of nonstationary time series. *Journal of the American Statistical Association* **93**(444), 1488–1501 (1998). DOI 10.1080/01621459.1998.10473808
2. Box, G.E.P., Jenkins, G.M., Reinsel, G.C., Ljung, G.M.: *Time Series Analysis: Forecasting and Control*. Wiley (2015)
3. Brockwell, P.J., Davis, R.A.: *Time Series: Theory and Methods*. Springer New York (1991). DOI 10.1007/978-1-4419-0320-4
4. Carter, C.K., Kohn, R.: Semiparametric Bayesian inference for time series with mixed spectra. *Journal of the Royal Statistical Society: Series B (Statistical Methodology)* **59**(1), 255–268 (1997). DOI 10.1111/1467-9868.00067
5. Choudhuri, N., Ghosal, S., Roy, A.: Bayesian estimation of the spectral density of a time series. *Journal of the American Statistical Association* **99**(468), 1050–1059 (2004). DOI 10.1198/016214504000000557
6. Cogburn, R., Davis, H.T.: Periodic splines and spectral estimation. *The Annals of Statistics* **2**(6), 1108–1126 (1974). DOI 10.1214/aos/1176342868
7. Dahlhaus, R.: Fitting time series models to nonstationary processes. *The Annals of Statistics* **25**(1), 1–37 (1997). DOI 10.1214/aos/1034276620
8. Duvenaud, D., Lloyd, J., Grosse, R., Tenenbaum, J., Ghahramani, Z.: Structure discovery in nonparametric regression through compositional kernel search. In: *Proceedings of the 30th International Conference on Machine Learning*, vol. 28, pp. 1166–1174 (2013)
9. Edwards, M.C., Meyer, R., Christensen, N.: Bayesian nonparametric spectral density estimation using B-spline priors. *Statistics and Computing* **29**(1), 67–78 (2019). DOI 10.1007/s11222-017-9796-9
10. Eilers, P.H.C., Marx, B.D.: Flexible smoothing with B-splines and penalties. *Statistical Science* **11**(2), 89–121 (1996). DOI 10.1214/ss/1038425655
11. Gangopadhyay, A., Mallick, B., Denison, D.: Estimation of spectral density of a stationary time series via an asymptotic representation of the periodogram. *Journal of Statistical Planning and Inference* **75**(2), 281–290 (1999). DOI 10.1016/s0378-3758(98)00148-7

12. Green, P.J.: Reversible jump Markov chain Monte Carlo computation and Bayesian model determination. *Biometrika* **82**(4), 711–732 (1995). DOI 10.1093/biomet/82.4.711
13. Gu, C.: *Smoothing Spline ANOVA Models*. Springer New York (2013). DOI 10.1007/978-1-4614-5369-7
14. Guo, W., Dai, M., Ombao, H.C., von Sachs, R.: Smoothing spline ANOVA for time-dependent spectral analysis. *Journal of the American Statistical Association* **98**(463), 643–652 (2003). DOI 10.1198/016214503000000549
15. Hadj-Amar, B., Rand, B.F., Fiecas, M., Lévi, F., Huckstepp, R.: Bayesian model search for nonstationary periodic time series. *Journal of the American Statistical Association* **115**(531), 1320–1335 (2019). DOI 10.1080/01621459.2019.1623043
16. Hastings, W.K.: Monte Carlo sampling methods using Markov chains and their applications. *Biometrika* **57**(1), 97–109 (1970). DOI 10.1093/biomet/57.1.97
17. James, N., Menzies, M.: COVID-19 in the United States: Trajectories and second surge behavior. *Chaos: An Interdisciplinary Journal of Nonlinear Science* **30**(9), 091102 (2020). DOI 10.1063/5.0024204
18. James, N., Menzies, M., Azizi, L., Chan, J.: Novel semi-metrics for multivariate change point analysis and anomaly detection. *Physica D: Nonlinear Phenomena* **412**, 132636 (2020). DOI 10.1016/j.physd.2020.132636
19. James, N., Menzies, M., Chan, J.: Changes to the extreme and erratic behaviour of cryptocurrencies during COVID-19. *Physica A: Statistical Mechanics and its Applications* **565**, 125581 (2021). DOI 10.1016/j.physa.2020.125581
20. Lu, J., Hoi, S.C., Wang, J., Zhao, P., Liu, Z.Y.: Large scale online kernel learning. *Journal of Machine Learning Research* **17**(47), 1–43 (2016)
21. Metropolis, N., Rosenbluth, A.W., Rosenbluth, M.N., Teller, A.H., Teller, E.: Equation of state calculations by fast computing machines. *The Journal of Chemical Physics* **21**(6), 1087–1092 (1953). DOI 10.1063/1.1699114
22. Paciorek, C.J., Schervish, M.J.: Nonstationary covariance functions for Gaussian process regression. In: *Proceedings of the 16th International Conference on Neural Information Processing Systems*, p. 273–280. MIT Press (2003)
23. Plagemann, C., Kersting, K., Burgard, W.: Nonstationary Gaussian Process regression using point estimates of local smoothness. In: *Machine Learning and Knowledge Discovery in Databases*, pp. 204–219. Springer Berlin Heidelberg (2008). DOI 10.1007/978-3-540-87481-2\_14
24. Rasmussen, C.E., Williams, C.K.I.: *Gaussian Processes for Machine Learning*. MIT Press (2005)
25. Roberts, G.O., Rosenthal, J.S.: General state space Markov chains and MCMC algorithms. *Probability Surveys* **1**(0), 20–71 (2004). DOI 10.1214/154957804100000024
26. Rosen, O., Stoffer, D.S., Wood, S.: Local spectral analysis via a Bayesian mixture of smoothing splines. *Journal of the American Statistical Association* **104**(485), 249–262 (2009). DOI 10.1198/jasa.2009.0118
27. Rosen, O., Wood, S., Stoffer, D.: *BayesSpec: Bayesian Spectral Analysis Techniques* (2017). URL <https://CRAN.R-project.org/package=BayesSpec>. R package version 0.5.3
28. Rosen, O., Wood, S., Stoffer, D.S.: AdaptSPEC: Adaptive spectral estimation for nonstationary time series. *Journal of the American Statistical Association* **107**(500), 1575–1589 (2012). DOI 10.1080/01621459.2012.716340
29. Todd, J.F.: Recommendations for nomenclature and symbolism for mass spectrometry. *International Journal of Mass Spectrometry and Ion Processes* **142**(3), 209–240 (1995). DOI 10.1016/0168-1176(95)93811-f
30. Todd, J.F.J.: Recommendations for nomenclature and symbolism for mass spectrometry (including an appendix of terms used in vacuum technology). (recommendations 1991). *Pure and Applied Chemistry* **63**(10), 1541–1566 (1991). DOI 10.1351/pac199163101541
31. Wahba, G.: Automatic smoothing of the log periodogram. *Journal of the American Statistical Association* **75**(369), 122–132 (1980). DOI 10.1080/01621459.1980.10477441
32. Wahba, G.: *Spline Models for Observational Data*. Society for Industrial and Applied Mathematics (1990). DOI 10.1137/1.9781611970128
33. Whittle, P.: On stationary processes in the plane. *Biometrika* **41**(3-4), 434–449 (1954). DOI 10.1093/biomet/41.3-4.434
34. Whittle, P.: Curve and periodogram smoothing. *Journal of the Royal Statistical Society: Series B (Methodological)* **19**(1), 38–47 (1957). DOI 10.1111/j.2517-6161.1957.tb00242.x
35. Wilson, A.G., Adams, R.P.: Gaussian process kernels for pattern discovery and extrapolation. In: *Proceedings of the 30th International Conference on International Conference on Machine Learning*, vol. 28, pp. 1067–1075 (2013)
36. Wood, S., Rosen, O., Kohn, R.: Bayesian mixtures of autoregressive models. *Journal of Computational and Graphical Statistics* **20**(1), 174–195 (2011). DOI 10.1198/jcgs.2010.09174
37. Wood, S.A., Jian, W., Tanner, M.: Bayesian mixture of splines for spatially adaptive nonparametric regression. *Biometrika* **89**(3), 513–528 (2002). DOI 10.1093/biomet/89.3.513
38. Wood, S.N.: P-splines with derivative based penalties and tensor product smoothing of unevenly distributed data. *Statistics and Computing* **27**(4), 985–989 (2017). DOI 10.1007/s11222-016-9666-x